Acta Neuropathol (1995) 89:126–138

REGULAR PAPER

S. A. L. Bennett · B. Stevenson · W. A. Staines
D. C. S. Roberts

Periodic acid-Schiff(PAS)-positive deposits in brain following kainic acid-induced seizures: relationships to *fos* induction, neuronal necrosis, reactive gliosis, and blood-brain barrier breakdown

Received: 9 May 1994 / Revised: 29 August 1994 / Accepted: 16 September 1994

Abstract Periodic acid-Schiff (PAS)-positive deposits have been demonstrated in the central nervous system (CNS) of patients suffering from a wide variety of neurodegenerative disorders including Alzheimer's disease, presenile dementia, Parkinson's disease, diabetes mellitus, myoclonic epilepsy, and cerebral palsy. The etiology of these deposits and their relationship to mechanisms of progressive neurodegeneration is unknown. In the present study, we demonstrate that the kainic acid model of limbic status epilepticus provides a useful system for the study of PAS-positive staining. The relationship between PAS-positive deposition, induction of *fos*-like immunoreactivity (FLI), neuronal necrosis, reactive gliosis, and blood-brain barrier breakdown following the kainic acid induction of status epilepticus was investigated. Epileptiform activity was elicited in rats by intraperitoneal administration of 10 mg/kg kainic acid and brains were examined 3, 5, 12, 24, 72, and 168 h after drug injection. Four distinct types of PAS-positive staining in rat brain were observed: type 1, extracellular matrix (ECM) or blood vessel associated-material; type 2, granular deposits; type 3, glial labelling; and type 4, neuronal labelling. Results demonstrated that the four types of PAS-positive staining were differentially associated with specific markers of neuropathology: (1) type 1 ECM staining and type 3 glia were preferentially localized to edematous tissue; (2) the majority of type 3 glia were identified as reactive astrocytes, while a minority of appeared to be proliferating microglia; (3) type 1 blood vessels labelled hemorrhaging vasculature; (4) early deposition of type 2 granules was predictive of subsequent cell loss; (5) chronic type 2 granular deposits and type 4 neuronal labelling not associated with cell death could be predicted by early changes in FLI; and (6) chronic deposition of all four forms of PAS-positive material was correlated with earlier, transient blood-brain barrier compromise. The results support the growing literature that local carbohydrate metabolism may be one of a constellation of parameters important to the development of progressive neurodegeneration.

Key words Neurodegeneration · Epilepsy · Kainic acid *fos* · Gliosis

Supported by a grant from the Medical Research Council (MRC) of Canada to D. C. S. R. and by an MRC Studentship to S. A. L. B.

S. A. L. Bennett
Department of Biochemistry, University of Ottawa, Ottawa, Ontario, Canada

B. Stevenson · D. C. S. Roberts (✉)
Department of Psychology, Carleton University, Ottawa, Ontario, Canada K1S 5B6
Tel.: (613)788-7495; Fax: (613)788-4052

W. A. Staines
Department of Anatomy and Neurobiology, University of Ottawa, Ottawa, Ontario, Canada

Introduction

The periodic acid-Schiff (PAS) reaction has been used clinically to identify progressive neurodegeneration in Alzheimer's disease [12, 19, 24, 26], presenile dementia [19, 24, 39], Parkinson's disease [5, 12], diabetes mellitus [32], myoclonic epilepsy [5], and cerebral palsy [10]. However, the chemical identity, etiology, and relative importance of these deposits to pathological mechanisms are unknown. The PAS reaction stains a variety of carbohydrate-containing components of both cells and the extracellular matrix (ECM), including glycogen, glycoproteins, glycolipids, sphingolipids, and some proteoglycans [7]. Dimedone (5,5-dimethyl-1,3-cyclo-hexanedione) can be used to improve the selectivity of the PAS reaction by blocking sugars that undergo only minimal oxidation during periodate treatment. This selection effectively reduces the amount of PAS-positive material in oxidized tissue, accentuating the reactivity of highly polymerized carbohydrates. PAS-dimedone (PAS-D)-positive material includes glycogen, highly sialated glycoproteins as, for example, members of the cell adhesion molecule (CAM) family, and heavily sialated glycolipids as, for example, members of the ganglioside family. Under such selective condi-

tions, pathological PAS-positive material has been noted in the central nervous system (CNS) of senescence-accelerated mice [1], aged cats [41] and dogs [40] and in the rodent brain following irradiation [43] or stab-wounding [15].

The kainic acid model of status epilepticus produces progressive neurodenegeration and long-term plastic alterations in limbic and other closely related brain regions. Cell death occurs as a consequence of sustained neuronal excitation, edema, inflammation, reactive gliosis, and blood-brain barrier breakdown [3, 4, 9, 22, 23, 27, 29, 38, 42]. These pathologies are also observed in clinical disorders. Focal sites of inflammation, activation of reactive astrocytes, and disruption of the blood-brain barrier are characteristic features of myoclonic epilepsy [22], Alzheimer's disease [2, 17, 18], Pick's disease [2], Creutzfeldt-Jakob degeneration [35], and multiple sclerosis [2, 33, 35]. In the present series of experiments, we have begun to explore the relationship between specific types of PAS-D staining and induction of *fos*-like immunoreactivity (FLI), neuronal loss, reactive gliosis, and blood-brain barrier breakdown in an attempt to establish temporal correlations between the development of PAS-D deposits and several other markers of brain damage.

Materials and methods

Induction of epileptiform seizures

Epileptiform seizures were induced in 41 male Wistar rats (Charles River, Canada), weighing 250–300 g. Subjects received intraperitoneal injections of either 10 mg/kg kainic acid (Sigma, USA) (n = 35) or physiological saline vehicle 1 ml/kg (n = 6). Rats were monitored for 10 h following drug injection and their behavior was rated according to previously published criteria [25]: 0, normal activity; 1, increased frequency of "freezing" and "wet-dog shakes"; 2, weak clonic convulsions with rearing; 3, increasingly severe convulsions with loss of postural control; 4, generalized limbic seizures; and 5, severe limbic seizures with respiratory difficulty. Three animals were implanted with electrodes and induction of epileptiform activity confirmed electrographically. All manipulations were carried out according to the strict ethical guidelines for animal experimentation established by the Medical Research Council of Canada. Subjects reaching stage 4 were anesthetized with sodium pentobarbital at 3, 5, 12, 24, 72, or 168 h after treatment (n = 5/time point) and were perfused with 60 ml of sodium phosphate-buffered saline (PBS: 10 m*M*, pH 7.2), followed by 120 ml of a modified Zamboni fixative (4% paraformaldehyde, 0.2% picric acid in 0.16 *M* phosphate buffer, pH 6.9). Brains were removed and postfixed for 4 h in the same fixative at 4°C and then transferred to 10% sucrose in 10 m*M* PBS for 24 h. Coronal sections, 15 μm in thickness, were cut on a cryostat and thaw-mounted on gelatin-coated microscope slides.

Morphological studies

Sections were routinely stained using either cresyl violet or hematoxylin eosin to assess morphological degeneration associated with seizure activity. Edematous tissue was identified as areas exhibiting macroscopic swelling of perineuronal and perivascular astroglia accompanied by neuropil vacuolization and herniation [22]. Swollen processes were confirmed as astroglial by Nissl staining sections immunoreacted with anti-glial fibrillary acidic protein (GFAP) as described below.

PAS-D staining

Sections were briefly hydrated and reacted at room temperature for 20 min in 0.5% periodic acid in distilled H_2O, dehydrated through progressively higher concentrations of ethanol, incubated for 1 h at 60°C in 5% dimedone in 100% ethanol, rehydrated through a descending series of ethanols, reacted for 20 min at room temperature in Schiff's reagent (14 m*M* parasanoline, 42.4 m*M* sodium bisulfite in 1 *M* HCl) and developed for 10 min in distilled H_2O. All chemicals were purchased from Sigma. Densitometry using a Zeiss scanning microscope attached to a Macintosh LC475 was performed on representative sections to determine the intensity of the reaction.

FLI and GFAP immunoreactivity

Sections were incubated with either a rabbit anti-*fos* antibody (1 : 500; Medac, USA) or a monoclonal mouse anti-GFAP antibody (1 : 40; Boehringer Mannheim, USA) overnight at 4°C. Primary and secondary antibodies were diluted in 10 m*M* PBS (pH 7.2) containing 0.3% Triton X-100. FLI was visualized by immunoperoxidase staining. Sections were washed repeatedly in PBS, incubated with biotinylated goat anti-rabbit antibodies (1 : 100; Amersham, USA), washed repeatedly in PBS, and incubated with streptavidin-horseradish peroxidase (1 : 100; Amersham) in PBS. Secondary and tertiary reactions were carried out at room temperature for 1 h. Immunoreactivity was developed by incubation in a 0.02% solution of 3,3′-diaminobenzidine tetrahydrochloride (Sigma) in 50 m*M* TRIS buffer (pH 7.4) followed by addition of H_2O_2 to a final concentration of 0.005%. GFAP immunoreactivity was assessed by immunofluorescence. Following incubation with anti-GFAP, sections were washed with PBS as above and reacted for 30 min at 37°C with FITC-labelled rabbit anti-mouse antibodies (1 : 20; Amersham) in PBS/Triton. Sections were coverslipped under glycerol containing 0.1% *p*-phenylenediamine. To assess specificity, adjacent sections were processed as described above but in the absence of primary antibody. Some sections were double-labelled with both anti-GFAP and PAS-D or anti-GFAP and either hematoxylin eosin or cresyl violet. These sections were incubated for 1 h with anti-GFAP antisera followed by fluorescence labelled secondary antibodies as described above. Because PAS-D staining is itself fluorescent under both FITC and rhodamine filters, anti-GFAP-labelled sections were examined and photographed prior to PAS-D processing. The short immunohistochemical incubation periods were required to preserve PAS-D reactivity and were sufficient to identify individual reactive astrocytes.

Blood-brain barrier breakdown

Blood-brain barrier breakdown was assessed by examining the extent of rat Ig extravasation into brain following kainic acid treatment essentially as described in [36]. Sections were incubated overnight at 4°C with a goat anti-rat Ig (1 : 100; Amersham) in PBS/Triton and processed for immunoperoxidase staining as described above.

Results

Kainic acid-induced seizures

Intraperitoneal injection of 10 mg/kg kainic acid induced stage 4 epileptiform activity within 2–3 h of treatment. The time course of seizure induction has been well characterized elsewhere [3, 4, 9, 22, 23, 27, 29, 38, 42]. Briefly, animals exhibited stage 1 'wet-dog shakes' 15–30 min after treatment. Stage 2 rearing and weak clonic convulsions were observed 60 min after injection. Rats

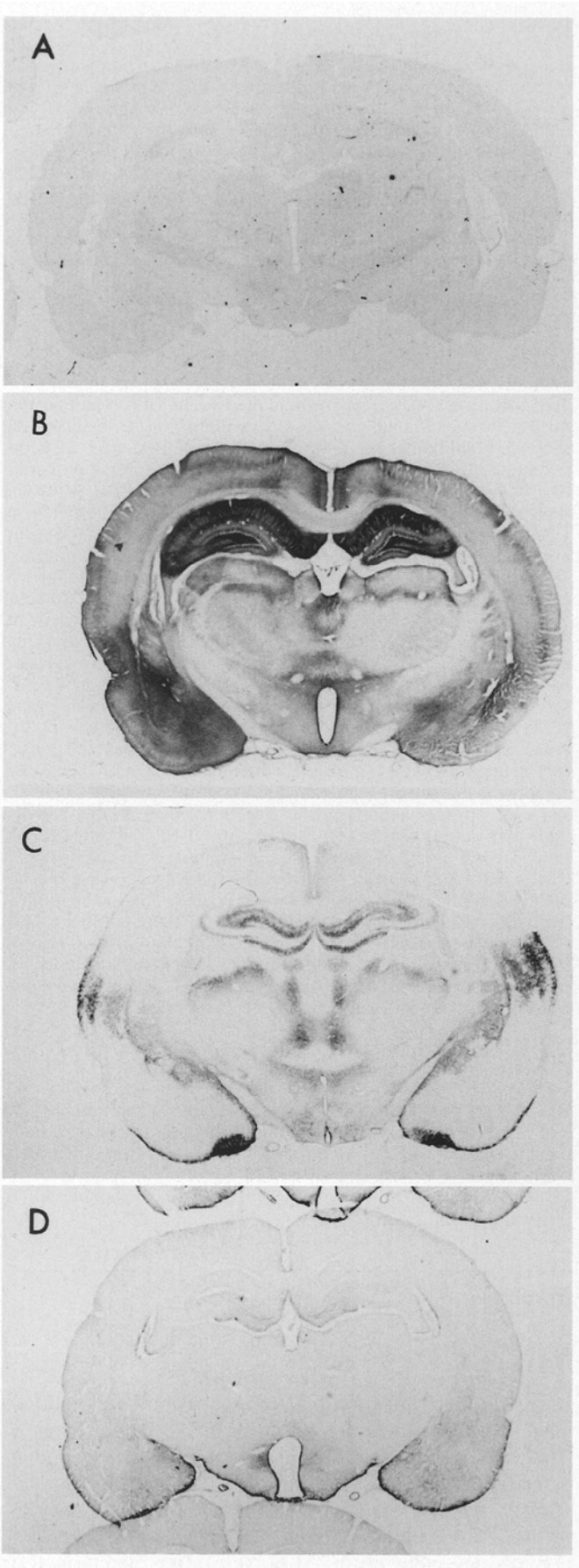

Fig. 1 The pattern of periodic acid-Schiff-dimedone (PAS-D) staining in control subjects 24 h after saline injection (**A**) or in kainic acid (10 mg/kg)-treated subjects at 24, 72, and 168 h after excitotoxin administration (**B–D**). Representative photomicrographs are depicted

demonstrated loss of postural control and increasingly severe stage 3 convulsions within 90 min of treatment, progressing rapidly to generalized stage 4 limbic seizures 120–180 min after excitotoxin administration with the exception of two animals that progressed to stage 5 within 130 min of treatment and were immediately sacrificed. No further investigation was conducted on these subjects. Behavioral indices of epileptiform activity continued for approximately 7 h in the remaining animals subsiding 12 h after kainate injection. Epileptiform activity was confirmed electrographically in three animals implanted with electrodes (data not shown). By 2 h after treatment, animals were exhausted, severely dehydrated, and showed signs of motoric impairment. Subjects exhibited normal food and water intake within 48–72 h of kainic acid injection and demonstrated normal locomotion 96 h after treatment. Rats receiving intraperitoneal injections of saline showed no adverse effects.

Accumulation of PAS-D positive material

Animals receiving intraperitoneal injections of saline did not exhibit any PAS-D positive staining at any time point. By contrast, animals treated with kainic acid exhibited time-dependent accumulation of PAS-D-positive material as depicted in Fig. 1. This accumulation was mapped and densitometry was performed on representative sections to determine the relative intensity of the PAS-D reaction over time. Increases are expressed as percent of background reactivity observed in saline-treated animals and are visually displayed in the graded shading of Fig. 2. Moderate reactivity was first detected 12 h after kainic acid treatment and was distributed diffusely throughout the brain. By 24 h after kainic acid administration intense PAS-D staining was distributed predominantly within limbic brain areas, most notably the piriform and entorhinal cortices, amygdaloid complex, hippocampal formation, specific thalamic nuclei, layers I and II of the neocortex, and throughout all of the layers of the perirhinal cortex. At 72 h after treatment, PAS-D-positive material was distributed in a penumbra of approximately 50–150 μm in width around areas exhibiting neurodegeneration (see below). At 168 h after kainic acid injection, lightly staining PAS-D-positive deposits were noted in the entorhinal cortex, layers I and II of the neocortex, around the third ventricle, and within the hippocampal formation.

As shown in Fig. 3, four different types of PAS-D positive material could be identified: type 1, ECM- and/or blood vessel-associated staining; type 2, granular depositions; type 3, glial-labelling; and type 4, neuronal-labelling. The time course of these deposits and their relationship to other markers of neuropathology are described below.

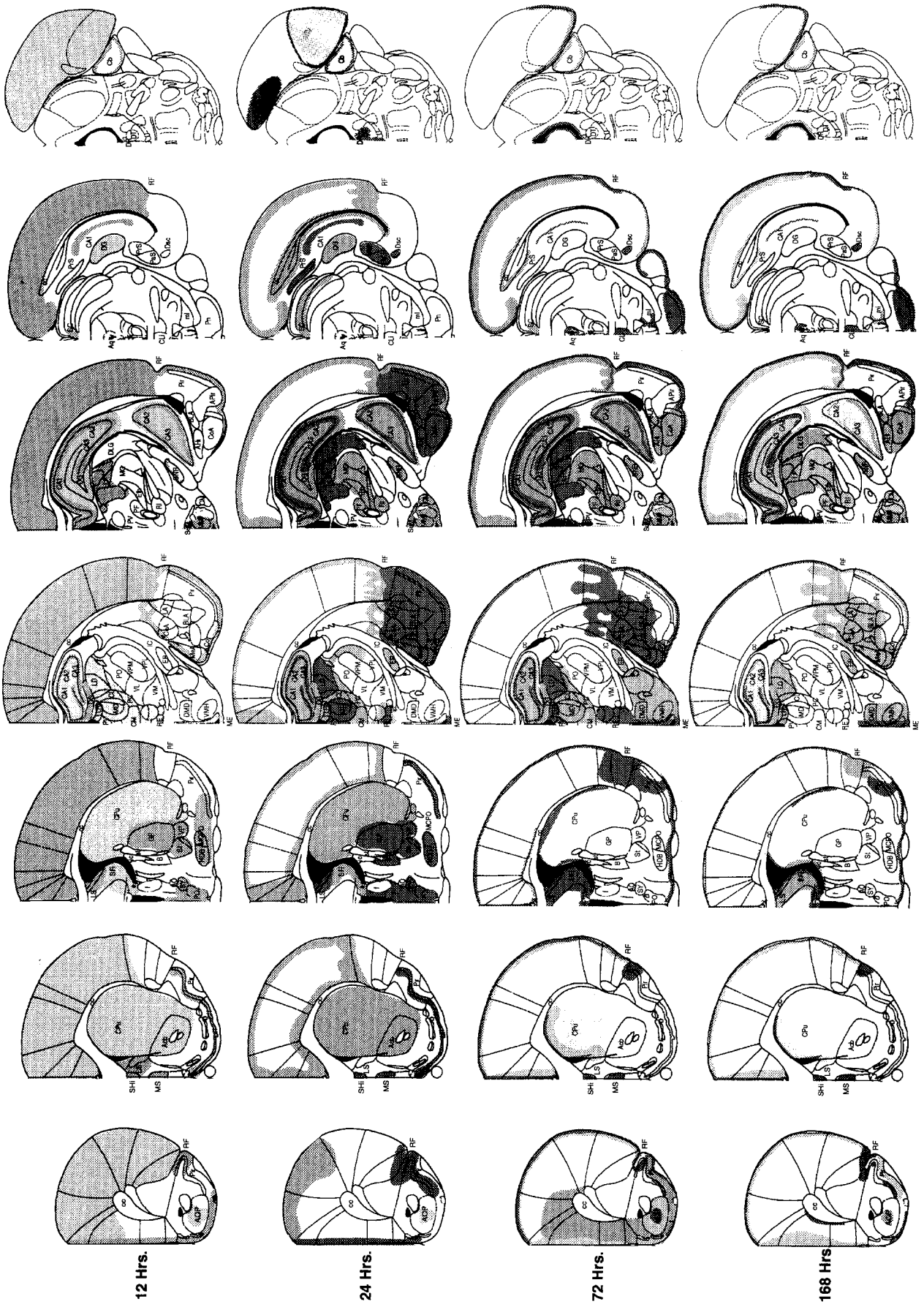

(for legend see next page)

◀ **Fig. 2** Pattern of PAS-D staining at 12, 24, 72, and 168 h after seizures induced by intraperitoneal injection of kainic acid (10 mg/kg). Staining was not detected at earlier time points. Drawings represents coronal sections localizing PAS-D stained material from a minimum of five rats per time period. Shading represents denistometric analysis of staining intensity. No attempt has been made to differentiate between types of PAS-D staining during densitometric analysis. Shading key: (▨) very light (25-fold increase over background); (▩) light (50-fold increase over background); (▩) moderate (100-fold increase over background); (■) intense (200-fold increase over background). (*cc* corpus callosum, *AOP* anterior olfactory posterior nucleus, *Pir* piriform cortex, *RF* rhinal fissure, *Shi* septohippocampal nucleus, *MS* medial septal nucleus, *CPu* caudate/putamen, *Acb* nucleus accumbens, *LS* lateral septal nucleus, *SFi* septal fimbrial nucleus, *f* fornix, *PO* preoptic nucleus, *AC* anterior commissure, *SY* striohypothalamic nucleus, *HDB* nucleus of horizontal limb diagonal band, *MCPO* magnocellular preoptic nucleus, *B* Bed nucleus, *st* stria terminalis, *VP* ventral pallidum, *GP* globus pallidum, *ic* internal capsule, *CA1–3* fields CA1–3 of Ammon's horn, *PV* paraventricular thalamic nucleus, *LhB* lateral habenular nucleus, *DG* dentate gyrus, *LD* lateral dorsal thalamic nucleus, *CL* centrolateral thalamic nucleus, *MD* mediodorsal thalamic nucleus, *CM* centromedial thalamic nucleus, *RE* reuniens thalamic nucleus, *DMD* dorsal medial hypothalamic nucleus, *VMH* ventromedial hypothalamic nucleus, *ME* median eminence, *PC* paracentral thalamic nucleus, *PO* posterior thalamic nucleus, *VPL* ventroposterolateral thalamic nucleus, *VPM* ventroposteromedial thalamic nucleus, *EB* entopeduncular nucleus, *CeA* central amygdaloid nucleus, *BLA* basolateral amygdaloid nucleus, *LA* lateral amygdaloid nucleus, MeA medial amygdaloid nucleus, *ACo* anterior cortical amygdaloid nucleus, *DLG* dorsal lateral geniculate, *LP* lateral posterior thalamic nucleus, *MG* medial geniculate nucleus, *PV* paraventricular nucleus, *PF* parafascicular nucleus, *Ri* rostral interstitial nucleus mlf, *Eth* ethnoid thalamic nucleus, *SNR* substantia nigra, *SuM* supramammillary nucleus, *MM* mediamammaillary nucleus, *AHi* amygdaloid hippocampal area, *APir* amygdaloid/piriform transition area, *SC* superior colliculus, *PRS* presubiculum, *PaS* parasubiculum, *DSC* lamina dissecans entorhinal area, *ml* medial leminiscus, *Pn* pontine nucleus, *Cli* caudal linear nucleus raphe, *DR* dorsal raphe nucleus, *DT* dorsal tegmental nucleus)

Neurodegeneration and PAS-D-positive deposits

Examination of Nissl-stained brain sections revealed two distinct phases of neuronal damage in subjects experiencing seizures. Data are presented in Table 1 for select midbrain structures. The first phase, 3–24 h after treatment, was characterized by the appearance of hyperchromatic, pyknotic neurons in around edematous tissue. Swollen astroglial processes in areas of neuropil vacuolization were anti-GFAP immunoreactive (described below). The degree of vacuolization within affected tissue increased with time as did the number of focal capillary hemorrhages preferentially localized to limbic structures. Blood vessel disruptions were assessed by extravasation of rat Ig into brain parenchyma around Nissl- and type 1-PAS-D delineated blood vessels (described below). By 12 h after treatment, large cystic cavities could be seen in the piriform and entorhinal cortices and entire cell fields within these areas were profoundly disrupted. Morphological alterations peaked with the cessation of epileptiform activity. By 24 h post-treatment, many neurons within affected areas had fragmented and hyperchromatic debris was observed throughout the hippocampal formation, thalamic nuclei, entorhinal and piriform cortices, and throughout the neocortex in the vicinity of the rhinal fissure. The degree of neuropil vacuolization and astroglial swelling was most pronounced at this time point. The second phase of neurodegeneration, 72–168 h after treatment, was characterized by a reduction in the degree of edema observed, morphological recovery of large numbers of affected neurons, accompanied, however, by permanent cell loss in discrete brain regions. By 168 h after kainic acid administration, lesions, consisting of small cystic cavities scattered throughout fields of large, hypochromatic neurons, were preferentially localized to discrete regions within the hippocampal formation, entorhinal and piriform cortices, and amygdaloid complex. Pyknotic and hyperchromatic neurons were rarely detected. In areas that had exhibited cell fragmentation, substantial cell loss was noted, most notably in CA1 and CA3 pyramidal cells of the hippocampal formation, throughout the piriform cortex and amygdaloid complex, and within the entorhinal cortex immediately surrounding the piriform cortex as previously reported [3, 4, 9, 22, 23, 27, 29, 38, 42].

The cellular distribution of PAS-D-positive material varied over time in parallel with the gross morphological alterations accompanying neurodegeneration (Table 2). Type 1 staining of blood vessels and ECM components and type 3 positive glia first appeared towards the end of epileptiform activity (12 h after treatment) and were preferentially localized to edematous tissue. The intensity of type 1 and type 3 staining peaked 24 h after kainic acid administration when cerebral edema was at its most pronounced and morphological alterations were the most extensive. Staining intensity decreased with time until, by 168 h after treatment, type 3 glial staining could only be observed within areas exhibiting residual edema.

While type 1 labelling of blood vessels and ECM and type 3 glial staining appeared to be correlated with the presence of edema, the appearance of type 2 granules was more indicative of subsequent cell death. PAS-D-positive granular deposits were first observed 24 h after treatment and were preferentially localized to regions that, at later time points, invariably exhibited cell loss. Staining disappeared prior to gross morphological evidence of necrosis until, by 168 h after induction of epileptiform activity, type 2 granules were absent from necrotic brain sites and could only be found in conjunction with type 1 ECM material forming a penumbra around damage tissue.

Type 4 neuronal staining was only observed 168 h after excitotoxin administration and was almost exclusively localized to regions of substantial cell loss with the exception of specific staining of striatal neurons in association with type 1 staining of ECM.

FLI and PAS-D-positive deposits

Epileptiform activity elicited neuronal expression of the *fos* family of proto-oncogenes (Table 2). Control subjects did not exhibit significant immunoreactivity (Fig. 4, panel A, B). FLI was observed early in the first phase of neurodegeneration and was highly predictive not only of cell

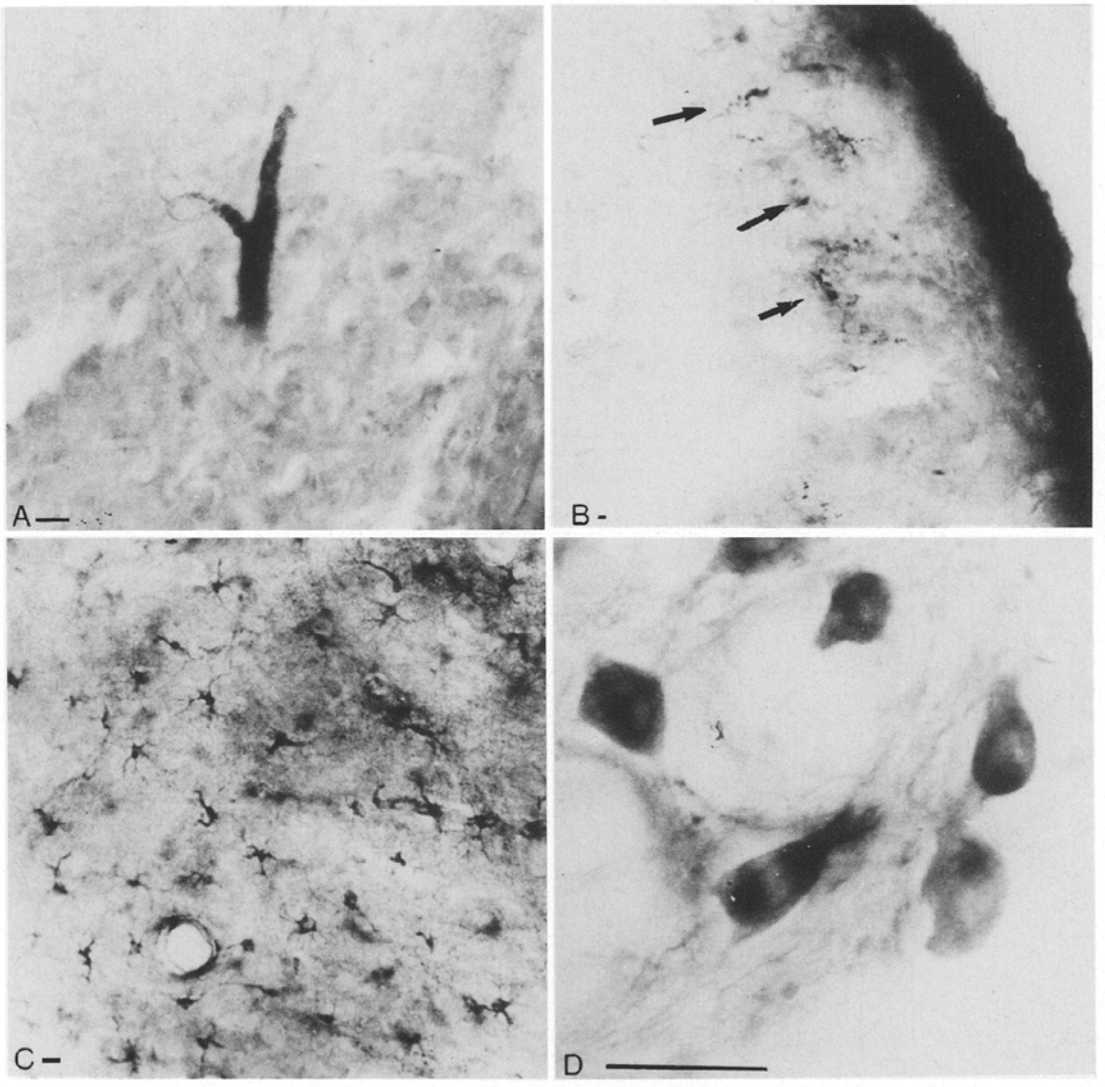

Fig. 3 A–D Photomicrographs of four different types of PAS-D-positive material found in rat brain following kainic acid (10 mg/kg)-induced seizures. **A** Type 1, blood vessel-associated staining 24 h after drug injection. Example taken from entorhinal cortex. **B** Type 1, extracellular matrix (ECM)-associated staining of layers I and II of the neocortex and type 2 granular depositions *(arrows)* 24 h after drug injection. Example taken from neocortex in the vicinity of the rhinal fissure. **C** type 3 glial labelling 24 h after drug injection. Example taken from entorhinal cortex. **D** type 4 neuronal labelling 168 h after drug injection. Example taken from dorsal striatum. **A–D** *Bars* = 40 μm

loss but also of later type 1 ECM, type 2 granular, and type 4 neuronal PAS-D staining. Of particular note is the temporal pattern of *fos*-like immunoreactivity observed in the hippocampal formation and piriform cortex. By 3 h after treatment, FLI was seen in neurons of the pyramidal cell layers of the hippocampal formation and within the dentate gyrus. Neurons in the piriform cortex also demonstrated intense labelling (Fig. 4, panels C, D). These areas corresponded to sites of type 4 neuronal labelling observed 168 h after treatment. By 5 h after drug injection, FLI was absent from both the CA4 and CA2 cell fields of the hippocampal formation and from the piriform cortex although immunoreactive cells could still be detected in the dentate gyrus, CA1 and CA3 of the hippocampus (Fig. 4, panels E, F), the amygdaloid complex, entorhinal cortex, layers I and II of the neocortex and throughout the cortical cell layers in the vicinity of the rhinal fissure, around the third ventricle, surrounding select thalamic nuclei, and, more anteriorly, along the dorsolateral border of the striatum. This distriubtion corresponded with residual type 1 ECM PAS-D staining observed 72 h after treatment and accurately predicted long-lasting type 2 granulr depositions and type 4 neuronal staining observed 168 h after treatment. By 24 h after treatment, FLI expression was no longer detected in the hippocampal formation with the exception of some weak staining in the dentate gyrus. FLI was absent from the entorhinal and piriform cortices but could be detected in the perirhinal region throughout areas that would express intense type 2 granular deposits 72 h after kainate administration. FLI reappeared 72 h after treatment in pyramidal cells of the hippocampal formation (but not in the dentate gyrus) and within neurons of the piriform cortex remaining immunoreactive 168 h post

Table 1 Morphological changes associated with kainic acid induced seizures

	Hyperchromatic, pyknotic cells						Cell fragmenttation						Cell loss						Edema, neurophil vacuolization					
Time (h):	3	5	10	24	72	168	3	5	10	24	72	168	3	5	10	24	72	168	3	5	10	24	72	168
Cortices:																								
Entorhinal cortex	+	++	+++	++++	+	+	–	–	–	+++	+	+	–	–	–	+	+++	++	++	+++	+++	++++	++	+
Piriform cortex	++	+++	+++	++++	++	–	–	–	++	+++	++	+	–	–	–	++	++++	++++	++	+++	+++	++++	++	+
Retrosplenial cortex	+	++	++	++	+	+	–	–	–	+	–	–	–	–	–	–	+	+	+	+	++	++	+	–
Parietal cortex	+	+	+	+	–	–	–	–	–	–	–	–	–	–	–	–	–	–	+	+	+	+	–	–
Perirhinal cortex	+	++	+++	++++	+	+	–	–	–	+++	+	+	–	–	–	+	++	+	++	+++	+++	+++	++	+
Hippocampus:																								
CA1	++	+++	+++	++++	++	+	–	–	++	+++	++	+	–	–	–	++	+++	++++	++	+++	+++	++++	++	+
CA2	++	+++	+++	++++	++	+	–	–	+	++	++	+	–	–	–	++	+++	+++	++	+++	+++	++++	++	+
CA3	++	+++	+++	++++	++	+	–	–	+	++	++	+	–	–	–	++	+++	+++	++	+++	+++	++++	++	+
CA4	++	++	++	+++	+	+	–	–	+	+	+	+	–	–	–	+	++	++	+	++	+++	+++	+	+
Dentate gyrus	+	+	+	++	+	–	–	–	–	–	–	–	–	–	–	–	+	+	+	++	++	+++	–	–
Amygdaloid nuclei:	–	++	+++	++++	++	+	–	–	++	+++	++	+	–	–	–	++	+++	++++	++	+++	+++	++++	++	+
Striatum:	–	–	–	–	–	–	–	–	–	–	–	–	–	–	–	–	–	–	–	–	+	+	–	–
Thalamic nuclei:																								
Medial dorsal	–	+	++	++	+	+	–	–	+	+	+	+	–	–	–	+	++	++	+	++	++	+++	+	–
Lateral dorsal	–	+	++	++	+	+	–	–	+	++	+	+	–	–	–	+	++	++	+	++	++	+++	+	–
Centrolateral	–	–	+	++	+	–	–	–	–	+	–	–	–	–	–	–	–	–	–	+	++	+++	+	–
Centromedial	–	–	+	++	+	–	–	–	–	+	–	–	–	–	–	–	–	–	–	+	++	+++	+	–
Ventrolateral	–	–	+	+	–	–	–	–	–	+	–	–	–	–	–	–	–	–	–	+	++	+++	+	–
Ventromedial	–	–	+	+	–	–	–	–	–	+	–	–	–	–	–	–	–	–	–	+	++	++	+	–
Reuniens	–	–	+	+	–	–	–	–	–	+	–	–	–	–	–	–	–	–	–	+	++	++	–	–

(– none; + to ++++ denotes increasing frequency/severity)

Table 2 Changes in PAS-D staining, FLI, anti-GFAP immunoreactivity, and blood-brain barrier breakdown (accumulation of rat Ig immunoreactivity) associated with kainic acid induced seizures (*PAS-D* periodic acid-Schiff-dimedone, *FLI* c-*fos*-like immunoreactivity, *1* type 1 extracellular matrix

	PAS-D						FLI						Anti-GFAP						Anti rat-IgG					
Time (h):	3	5	10	24	72	168	3	5	10	24	72	168	3	5	10	24	72	168	3	5	10	24	72	168
Cortices:																								
Entorhinal cortex	–	–	1,3	1,3	1,3	1,3	++	–	–	–	++	++	+	++	+++	++++	++	+	+	+	++	++++	+	–
Piriform cortex	–	–	1,3	1,2,3	1,3	1,3,4	+++	–	–	–	+++	+++	+	++	+++	++++	++	+	+	+	++	++++	++	+
Retrospelnial cortex	–	–	1,3	1,3	1,3	1,3	+	+	+	–	–	–	+	+	++	+++	+	–	+	+	+	++	+	–
Parietal cortex	–	–	1,3	1,3	1	1	+	+	+	–	–	–	+	+	+	++	–	–	+	+	+	++	–	–
Perirhinal cortex	–	–	1,3	1,3	1,2,3	1–4	++	++	+	++	–	–	+	+	++	+++	+	+	+	+	++	+++	++	–
Hippocampus:																								
CA1	–	–	1,3	1,2,3	1,3	1,3,4	+	+	+	+	++	++	+	++	+++	++++	++	+	+	+	++	++++	+	+
CA2	–	–	1,3	1,3	1,3	1,3,4	+	+	+	+	+	+	+	++	+++	++++	++	+	+	+	++	++++	–	–
CA3	–	–	1,3	1,2,3	1,3	1,3,4	++	+	+	–	++	++	+	++	+++	++++	++	+	+	+	++	++++	+	+
CA4	–	–	1,3	1,3	1,3	1,3,4	++	–	–	–	+	+	+	++	+++	++++	++	+	+	+	++	++++	–	–
Dentate gyrus	–	–	1,3	1,3	1	1,4	++	+	+	+	–	–	+	+	++	+++	+	+	+	+	++	++++	+	–
Amygdaloid nuclei	–	–	1,3	1,2,3	1,3	1,3,4	++	+	–	–	++	++	+	++	+++	++++	–	–	+	+	++	++++	+	+
Striatum	–	–	–	1	1	1,4	+	+	+	+	++	++	–	+	+	–	–	–	+	+	+	+	–	–
Thalamic nuclei:																								
Medial dorsal	–	–	1,3	1,3	1,3	1	+	+	+	+	–	–	+	+	++	+++	–	–	+	+	+	–	–	–
Lateral dorsal	–	–	1,3	1,3	1,3	1	1	+	+	+	–	–	+	+	++	+++	–	–	+	+	+	–	–	–
Centrolateral	–	–	1,3	1,3	1	1	+	+	+	+	–	–	+	+	++	+++	–	–	+	+	+	–	–	–
Centromedial	–	–	1,3	1,3	1	1	+	+	+	+	–	–	+	+	++	+++	–	–	+	+	+	–	–	–
Ventrolateral	–	–	1	1,3	1	–	+	+	+	–	–	–	+	+	++	+++	–	–	+	+	+	–	–	–
Ventromedial	–	–	1	1,3	1	–	+	+	+	–	–	–	+	+	++	+++	–	–	+	+	+	–	–	–
Reuniens	–	–	1	1,3	1	–	+	+	+	–	–	–	+	+	++	+++	–	–	+	+	+	–	–	–

(– none; + to ++++ denotes increasing frequency/severity)

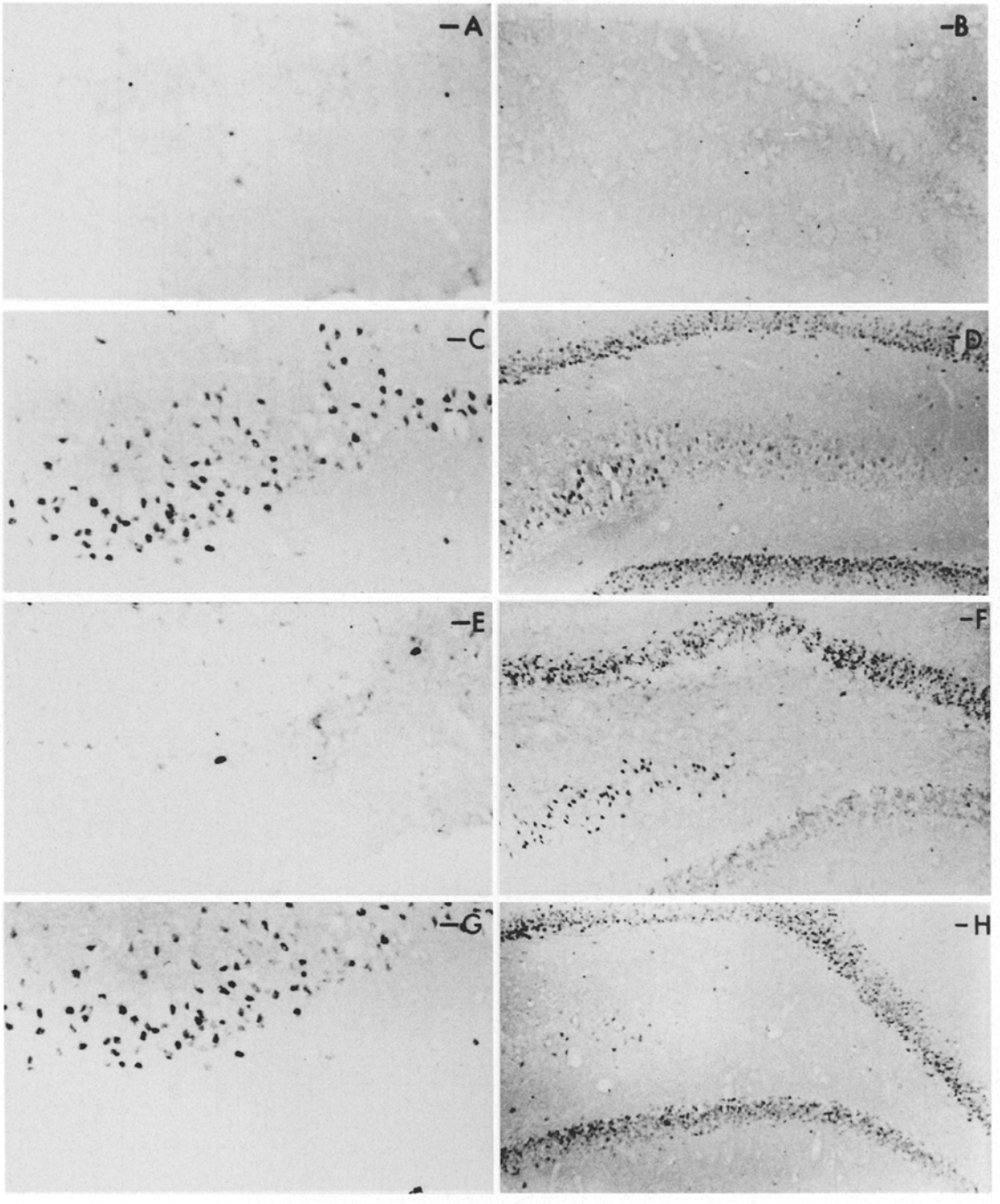

Fig. 4 c-*fos*-like immunoreactivity in control subjects 3 h after saline injection (**A, B**) and kainic acid (10 mg/kg)-treated animals 3 h (**C, D**) and 5 h (**E, F**) and 24 h (**G, H**) after drug injection. **A, C, E, G** are taken from the piriform cortex. **B, D, F, H** are taken from the hippocampal formation. **A–H** *Bars* = 80 μm

treatment (Fig. 4, panels G, H). These areas demonstrated considerable cell death and chronic accumulation of type 1 ECM and type 4 neuronal PAS-D staining. Finally, FLI could also be detected 72 h after kainate injection in a discrete areas of the dorsolateral striatum; a region exhibiting intense type 4 neuronal labelling 168 h after seizure induction without showing any signs of cell loss.

GFAP immunoreactivity and PAS-D-positive deposits

Reactive gliosis, as assessed by GFAP immunoreactivity, was evident 3 h after treatment and was largely confined to the proximity of large blood vessels (Table 2). By 5 h after treatment, intense GFAP-labelling was evident throughout the hippocampal formation, the entorhinal and piriform cortices, and neocortical cell layers in the vicinity of the rhinal fissure. Swollen astroglial processes in areas of neuropil vacuolization were anti-GFAP immunoreactive. There was a substantial increase in GFAP immunoreactivity 24 h after treatment (Fig. 5, panel A) and this increase correlated with both the appearance of type 3

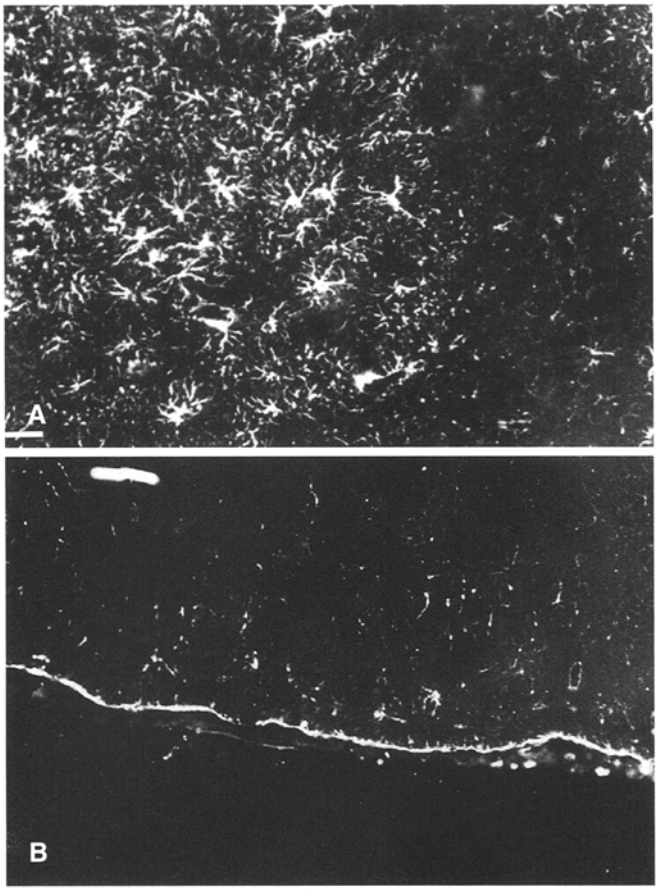

Fig. 5 Photomicrographs of anti-GFAP immunoreactive glia after kainic acid (10 mg/kg) administration. **A** depicts staining in the hippocampal formation 24 h after drug injection. **B** depicts residual labelling in the entorhinal cortex 72 h after excitotoxin administration. *Bar* = 20 μm

PAS-D astrocytes within identical areas and with the increase in neuropil disruption and tissue vacuolization. Double labelling with PAS-D and GFAP confirmed that the majority of PAS-D-positive cells observed throughout regions of profound edema were reactive astrocytes, although not all GFAP-reactive astrocytes were PAS-D positive. A minority of type 3-labelled glial cells were GFAP negative and had the morphological appearance of microglia. By 72-168 h after treatment, PAS-D-positive, GFAP-immunoreactive astrocytes were confined to the neocortical layers in and around the rhinal fissure, within small portions of the hippocampus, and scattered sporadically throughout the entorhinal cortex (Fig. 5, panel B).

Blood-brain barrier breakdown and PAS-D-positive deposits

Increases in blood-brain barrier permeability were assessed by extravasation of rat Ig into brain parenchyma (Table 2). In sections from control brain, only vessels in the circumventricular organ such as the arcuate nucleus and the median emminence showed permeability to blood Ig and in

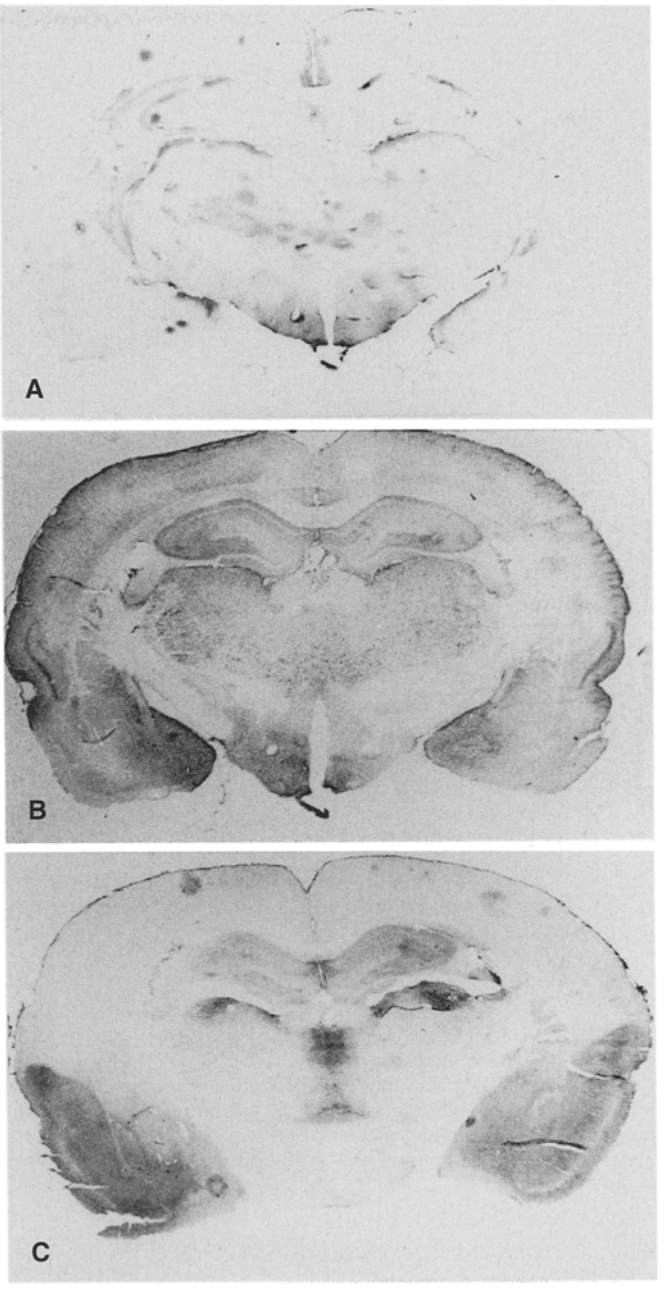

Fig. 6 The pattern of blood-brain barrier breakdown after kainic acid (10 mg/kg)-induced epileptiform activity. Representative photomicrographs illustrate the extent of rat Ig extravasation into brain parenchyma 3, 12, and 24 h (**A–C**) after drug injection

these loci there was no associated PAS-D staining. Within 3–5 h of kainate administration, rats demonstrated a large number of focal hemorrhages distributed randomly throughout the brain (Fig. 6, panel A). By 12 h after treatment, the distribution of Ig immunoreactivity had changed (Fig. 6, panel B). Staining was no longer confined to damaged blood vessels but was also detected throughout the perirhinal, piriform and entorhinal cortices in a pattern congruent with that of type 1 ECM and type 3 glial PAS-D staining observed at the same time point. Blood vessels in areas

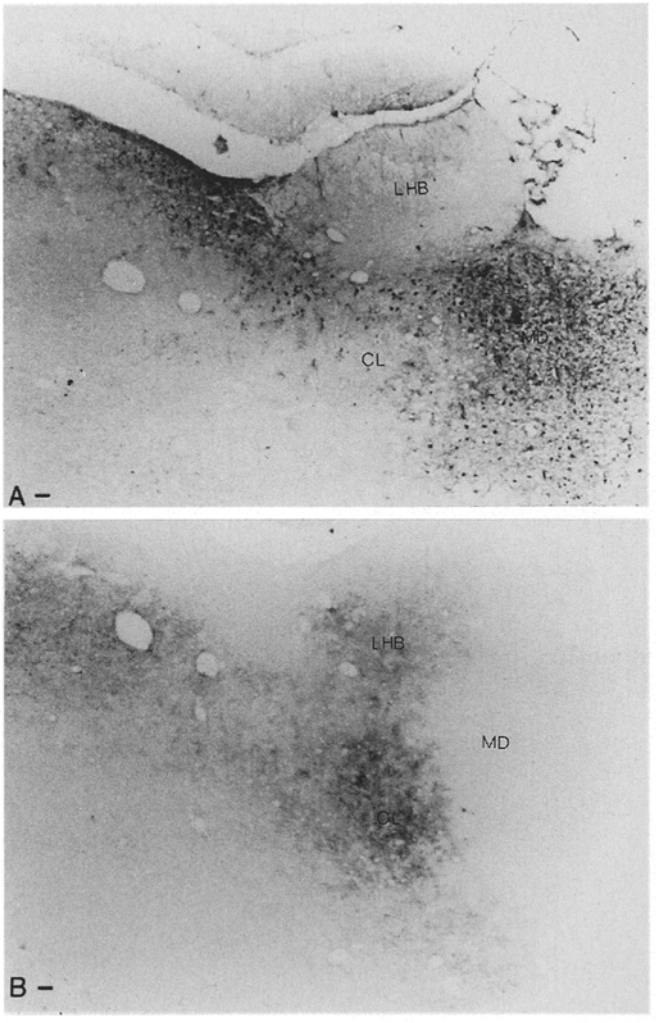

Fig. 7 Relationship between neuronal-labelling of cells with rat Ig (**A**) and type 1 ECM accumulation of PAS-D staining (**B**) 24 h after kainic acid (10 mg/kg) administration. Representative photomicrographs depict a single section stained for both rat Ig immunoreactivity and PAS-D staining. Abbreviations as in Fig. 1. **A, B** Bars = 200 μm

that had exhibited focal extravasation of rat Ig were type 1 PAS-D positive. Some neurons in the hippocampal formation, centromedial, laterodorsal and reuniens nuclei, piriform cortex, and throughout layers I and II of the neocortex had taken up blood proteins and as such were Ig immunoreactive. Many of these Ig-positive cells were surrounded by PAS-D type 2 granules.

The intensity of rat Ig labelling peaked 24 h after treatment. Staining was detected only in limbic structures and could no longer be observed to surround damaged blood vessels (Fig. 6, panel C). Double labelling demonstrated that PAS-D-positive deposits either surrounded areas containing cells which had taken up Ig (Fig. 7, Panel A and B) or overlapped areas exhibiting diffuse rat Ig labelling (i.e., the hippocampal formation and entorhinal cortex). Immunoreactivity dissipated with time until, by 72 h after treatment, rat Ig could only be detected in the piriform cortex and hippocampal formation. By 168 h after treatment, brain sections of kainate-treated subjects were equivalent to control with the exception of the some residual labelling in the piriform cortex.

Discussion

The kainic acid model of epileptiform activity consistently results in a time-dependent accumulation of PAS-D-positive material in rat brain. Four distinct types of deposits can be resolved: type 1, ECM- and blood vessel-associated material; type 2, granular deposits; type 3, glial labelling; and type 4, neuronal labelling. These deposits are similar in morphology to those detected in the human CNS of patients with Alzheimer's disease [12, 19, 24, 26], presenile dementia [19, 24, 39], Parkinson's disease [5, 12], diabetes mellitus [32], myoclonic epilepsy [5], and cerebral palsy [10]. In an attempt to provide insight into the nature of these deposits, we have examined the relationship between PAS-D-positive staining and the development of edema, reactive gliosis, neuronal loss, and blood-brain barrier breakdown during kainic acid-induced limbic status epilepticus.

Two stages of nerve cell damage were observed following induction of epileptiform activity with kainic acid; an acute phase (3–24 h after treatment), characterized by the appearance of edema and the presence of hyperchromatic, pyknotic, and fragmenting neurons, and a chronic phase (72–168 h after treatment), characterized both by a marked improvement in acute parameters of neurodegeneration and substantial cell loss in discrete brain regions. Identification of these stages is consistent with previous studies of excitotoxin neurodegeneration [3, 4, 9, 17, 22, 23, 27–31, 38, 42]. These morphological changes were accompanied by two phases of reactive gliosis and blood-brain barrier breakdown [34]. In the acute phase, blood-brain barrier breakdown, as assessed by extravasation of rat Ig molecules into brain parenchyma, was distributed randomly throughout the brain around hemorrhaging blood vessels (medium and fine caliber). Early reactive gliosis was initially confined to the vicinity of disrupted vasculature. With time, extensive GFAP immunoreactivity could be observed throughout edemic tissue in and around areas of blood-brain barrier breakdown. PAS-D staining was first observed towards the end of the acute phase. Type 3 staining of glial cells could be observed throughout edematous tissue. The majority of these PAS-D-positive cells were identified as GFAP-immunoreactive astrocytes, while a small subpopulation were GFAP negative and morphologically characteristic of microglia. The appearance of PAS-D-positive staining correlated with the induction of a diffuse spread of blood proteins throughout specific limbic structures. Initially, labelling type 1 of the ECM could be observed throughout area of blood-brain barrier breakdown, while specific labelling of hemorrhaging vasculature could be detected around rat Ig-positive capillaries. However, towards the end of the acute phase of neurodegeneration, type 1 ECM staining formed a penumbra around areas exhibiting serum protein accumu-

lation, while type 2 granular deposits were localized within Ig-reactive tissue in specific association with Ig-positive neurons. This distribution of type 2 granular deposits was highly predictive of subsequent neuronal death observed in the chronic phase of neurodegeneration. In this later phase of damage, tissue was no longer grossly edematous. Rat Ig immunoreactivity was minimal and confined to areas of residual edema and type 3 reactive gliosis. Substantial cell death was noted in areas that had exhibited type 2 granular deposits during the acute phase of neurotoxicity and was surrounded by a penumbra of approximately 100 μm in width of type 1 ECM material. The few remaining cells within these regions were morphologically intact, but were hypochromatic. Many of these neurons were type 4 PAS-D positive.

Surprisingly, early induction of the *fos* family of proto-oncogenes was found to be highly predictive not only of subsequent cell death but also of type 2 granular deposits and type 4 neuronal labelling. *fos* genes are members of the early response gene family that encodes for transcription factors. During epileptiform seizures and other disorders, their gene products are believed to couple neuronal excitation to changes in target gene expression [6, 8, 11, 13, 14, 16, 20, 21, 31]. Early and long-lasting induction of the protein (1–5 h after seizure induction) can be used to determine the degree and extent of prolonged neuronal excitation and, hence, identify neuronal populations most likely to exhibit subsequent cell loss. In addition, it has recently been demonstrated that renewed expression of c-*fos* mRNA is also observed in apoptotic cell populations 72–168 h after kainate administration [37]. The results of the present study are in accordance with these observations. However, in addition to cell death, FLI could also be used to predict PAS-D neuropathology. For example, FLI labelling was detected 24 h after treatment in the perirhinal region immediately surrounding damaged portions of the entorhinal cortex as well as 72 h after treatment in discrete regions of the lateral striatum; areas that do not exhibit cell loss. The distribution accurately predicted the appearance of type 2 granular deposits 72 h after kainate injection and specific populations of type 4 labelled neurons observed 168 h after treatment. These results indicate that FLI is indicative both of cell loss and accumulation of PAS-D-positive material. FLI may be either a coincident byproduct of the breakdown in cell signalling observed after kainic acid-induced seizures or may actually be a required component in a gene regulation pathway mediating both neuronal death and aberrant carbohydrate accumulation.

The identity of the PAS-D-positive components in diseased brain remains ambiguous. The PAS-D stain is known to be specific for highly polymerized carbohydrates such as glycogen or highly sialated glycoproteins and glycolipids [7]. We have noted that type 2 granules and type 4 neurons are resistant to amylase digestion (unpublished data), suggesting that this material is unlikely to be glycogen. These observations are in accordance with Akiyama et al. [1], who demonstrated that the PAS-D-positive granular depositions observed in the brain of senescence-accelerated mice were amylase resistant and histochemically uncharacteristic of glycogen polymers. Further studies are required to identify the carbohydrate components of the PAS-D-positive material with any certainty.

Aberrant PAS-D-positive material has been detected in the brain of patients with Alzheimer's disease [19, 24], presenile dementia [19, 24, 39], Parkinson's disease [5], diabetes mellitus [32], myoclonic epilepsy [5], and cerebral palsy [10], as well as in the brain of senescence accelerated mice [1] and in the CNS of experimental animals following following X- and gamma-irradiation [43] and stab wounding [15], suggesting that local carbohydrate metabolism is associated with progressive neurodegeneration. The present study describes the relationship between PAS-D staining and induction of FLI, neuronal necrosis, reactive gliosis, and blood-brain barrier breakdown in an attempt to establish temporal correlations between the development of PAS-D deposits and several other markers of brain damage using a well-characterized animal model of neuropathology. We have identified four types of aberrant PAS-D material in rat brain following kainic acid induced seizures: type 1, ECM or blood vessel associated-material; type 2, granular deposits; type 3, glial labellling; and type 4, neuronal labelling. Results demonstrate that (1) type 1 ECM staining and type 3 glia are preferentially localized to edematous tissue; (2) the majority of type 3 glia are reactive astrocytes, while a minority of PAS-positive glia appear to be proliferating microglia; (3) type 1 blood vessels identify hemorrhaging vasculature; (4) the early distribution of type 2 granules accurately predicts subsequent cell loss; (5) chronic type 2 granular deposits and type 4 neuronal labelling not associated with cell death are predicted by early changes in FLI; and (6) chronic deposition of all four forms of PAS-positive material is confined to areas that exhibited substantial, transient blood-brain barrier compromise. We suggest that the increase in PAS-D staining represents either the synthesis of heavily glycosylated constituent(s) of the ECM by both neurons and astrocytes in response to blood-brain barrier breakdown or the accumulation of serum glycoproteins extravasating through a compromised blood-brain barrier. The kainic acid model of neurodegeneration may assist us in identifying the PAS-positive deposits associated with chronic neurodegeneration as well as provide a means of determining their relative importance in human progressive neurodegenerative disorders.

Acknowledgement The authors thank J. Bennett for skilful technical assistance.

References

1. Akiyama H, Kamayama M, Akiguchi I, Sugiyma H, Kawamata T, Fukuyama H, Kimura H, Matsushita M (1986) Periodic acid-Schiff (PAS)-positive granular structures increase in the brain of senescence-accelerated mouse (SAM). Acta Neuropathol (Berl) 72:124–129
2. Akiyama H, Kawamata T, Yamada T, Tooyama I, Ishii T, McGeer PL (1993) Expression of intercellular adhesion molecule (ICAM)-1 by a subset of astrocytes in Alzheimer disease and some other degenerative neurological disorders. Acta Neuropathol 85:628–634

3. Ben-Ari Y (1983) The role of seizures in kainic acid induced brain damage. In: Fuxe K, Roberts P, Schwartz R (eds) Excitotoxins: Wenner Gren International Symposium. Macmillan Press, London, pp 184–198
4. Ben,Ari Y, Tremblay EP, Ottersen OP, Meldrum BS (1980) The role of epileptic activity in hippocampus and 'remote' cerebral lesions induced by kainic acid. Brain Res 191:79–97
5. Cajal RS, Glanes A, Martinez A, Saenz E, Gutierrez M (1974) Lafora's disease: an ultrastructural and histochemical study. Acta Neuropathol (Berl) 30:189–196
6. Clark M, Post RM, Weiss SRB, Nakajima T (1992) Expression of c-fos mRNA in acute and kindled cocaine seizures in rats. Brain Res 582:101–106
7. Culling CFA (1974) Handbook of histopathological techniques and histochemistry. Thomas Burton, London
8. Daval J-L, Nakajima T, Gleiter CH, Post RM, Marangos PJ (1989) Mouse brain c-fos mRNA distribution following a single electroconvulsive shock. J Neurochem 52:1954–1957
9. Dawson R Jr, Wallace DR (1992) Kainic acid-induced seizures in aged rats: neurochemical correlates. Brain Res Bull 29:459–468
10. Leon GA de (1974) Bielschowsky bodies: Lafora-like inclusions associated with atrophy of the lateral pallidum. Acta Neuropathol (Berl) 30:183–188
11. Duman RS, Craig JS, Winston SM, Deutch AY, Hernandez TD (1992) Amygdala kindling potentiates seizure-stimulated immediate-early gene expression in rat cerebral cortex. J Neurochem 59:1753–1760
12. Forno LS, Langston JW (1993) Lewy bodies and aging: relation to Alzheimer's and Parkinson's diseases. Neurodegeneration 2:19–24
13. Gass P, Herdegen T, Bravo R, Kiessling M (1992) Induction of immediate early gene encoded proteins in the rat hippocampus after bicuculline-induced seizures: differential expression of KROX-24, FOS and JUN proteins. Neuroscience 48:315–324
14. Gass P, Herdegen T, Bravo R, Kiessling M (1993) Spatiotemporal induction of immediate early genes in the rat brain after limbic seizures: effects of NMDA receptor antagonist MK-801. Eur J Neurosci 5:933–943
15. Guth L, Dempsey PJ (1970) Mechanisms controlling glycogen levels in injured brain, normal brain, liver and heart. Exp Neurol 29:152–161
16. Herdegen T, Sandkühler J, Gass P, Kiessling M, Bravo R, Zimmermann M (1993) JUN, FOS, KROX, and CREB transcription factor proteins in the rat cortex: basal expression and induction by spreading depression and epileptic seizures. J Comp Neurol 333:271–288
17. Kalaria RN (1993) The immunopathology of Alzheimer's disease and some related disorders. Pathology 13367:12336–13105
18. Kalaria RN, Grahovac I (1990) Serum amyloid P immunoreactivity in hippocampal tangles, plaques and vessels: implications for leakage across the blood-brain barrier in Alzheimer's disease. Brain Res 516:39–353
19. Kobayashi K, Miyazu K, Fukutani Y, Nakamura I, Yamaguchi N (1992) Gallyas-Schiff stain for senile plaques. Biotech Histochem 67:256-260
20. Labiner DM, Butler LS, Cao Z, Hosford DA, Shin C, McNamara JO (1993) Induction of c-fos mRNA by kindled seizures: complex relationship with neuronal burst firing. J Neurosci 13:744–751
21. Lanaud P, Maggio R, Gale K, Grayson DR (1993) Temporal and spatial patterns of expression of c-fos, zif/268, c-jun and jun-B mRNAs in rat brain following seizures evoked focally from the deep prepiriform cortex. Exp Neurol 119:20–31
22. Lassman H, Petsche U, Kitz K, Baran H, Sperk G, Seitelberger F, Hornikiewitz O (1984) The role of brain edema on epileptic brain damage induced by systemic kainic acid injection. Neuroscience 13:671–704
23. Lothman EW, Collins RC (1981) Kainic acid induced limbic seizures: Metabolic, behavioural, encephalographic, and neuropathological correlates. Brain Res 218:299–318
24. Mann DM, Sumpter PQ, Davies CA, Yates PO (1987) Glycogen accumulates in the cerebral cortex in Alzheimer's disease. Acta Neuropathol (Berl) 73:181–185
25. McIntyre D, Nathanson D, Edson N (1982) A new model for partial status epilepticus based on kindling. Brain Res 250:53–63
26. McKeith I, Fairbairn A, Briel R, Harrison R, Tasker N (1993) Lewy bodies and Alzheimer's disease. Br J Psychiatry 163:262–263
27. Nadler JV, Cuthbertson GJ (1980) Kainic acid neurotoxicity toward hippocampal formation: Dependence on specific excitatory pathways. Brain Res 195:47–56
28. Ogawa M, Araki M, Nagatsu I, Yoshida M (1989) Astroglial cell alteration caused by neurotoxin: immunohistochemical observations with antibodies to glial fibrillary acidic protein, laminin, and tyrosine hydroxylase. Exp Neurol 106:187–196
29. O'Shaughnessy D, Gerber GJ (1986) Damage induced by systemic kainic acid in rats is dependent upon seizure activity – A behavioral and morphological study. Neurotoxicology 7:187–202
30. Paulus W, Jellinger K (1993) Comparison of integrin adhesion molecules expressed by primary brain lymphomas and nodal lymphomas. Acta Neuropathol 86:360–364
31. Popovici T, Represa A, Crépel V, Barbin G, Beaudoin M, Ben-Ari Y (1990) Effects of kainic acid-induced seizures and ischemia on c-*fos*-like proteins in rat brain. Brain Res 536:183–194
32. Powell HC, Ward HW, Garrett RS, Orloff MJ, Lampert PW (1979) Glycogen accumulation in the nerves and kidney of chronically diabetic rats. J Neuropathol Exp Neurol 38:114–127
33. Rieckmann P, Nünke K, Burchhardt M, Albrecht M, Wiltfang J, Ulrich M, Felgenhauer K (1993) Soluble intercellular adhesion molecule-1 in cerebrospinal fluid: an indicator for the inflammatory impairment of the blood-cerebrospinal fluid barrier. J Neuroimmunol 47:133–140
34. Saija A, Princi P, Pisani A, Santoro G, De Pasquale R, Massi M, Costa G (1992) Blood-brain barrier dysfunctions following systemic injection of kainic acid in the rat. Life Sci 51:467–477
35. Schluesener HJ, Meyermann R (1993) Intercrines in brain pathology. Expression of intercrines in a multiple sclerosis and Morbus Creutzfeldt-Jakob lesion. Acta Neuropathol 86:393–396
36. Schmidt-Kastner R, Meller D, Bellander B-M, Strömberg I, Olson L, Ingvar M (1993) A one-step immunohistochemical method for detection of blood-brain barrier disturbances for immunoglobulins in lesioned rat brain with special reference to false-positive labelling in immunohistochemistry. J Neurosci Methods 46:121–132
37. Smeyne RJ, Vendrell M, Hayward M, Baker SJ, Miao GG, Schilling K, Robertson LM, Curran T, Morgan JI (1993) Continuous c-*fos* expression precedes programed cell death in vivo. Nature 363:166–169
38. Sperk G, Lassman H, Baran H, Seitelberger F, Hornikiewicz O (1985) Kainic acid-induced seizures: dose-relationship of behavioural, neurochemical, and histopathological changes. Brain Res 338:289–295
39. Suzuki K, David E, Kutschman B (1971) Presenile dementia with "Lafora-like" intraneuronal inclusions. Arch Neurol 25:69–80
40. Suzuki Y, Akiyama K, Suu S (1978) Lafora-like inclusion bodies in the CNS of aged dogs. Acta Neuropathol (Berl) 44:217–222
41. Suzuki Y, Kamiya S, Ohta K, Suu S (1979) Lafora-like bodies in a cat. Acta Neuropathol (Berl) 48:55–58
42. Sztriha L, Joo F (1986) Intraendothelial accumulation of calcium in the hippocampus and thalamus of rats after systemic kainic acid administration. Acta Neuropathol (Berl) 72:111–116
43. Wolfe LS, Klatzo I, Mizuel J, Tobias C, Haymaker W (1962) Effect of alpha-particle irradiation on brain glycogen in the rat. J Neurochem 9:213–218